

## Growth of ( $\alpha$ Ti) Grain-Boundary Layers in Ti–Co Alloys

A. S. Gornakova<sup>a, \*</sup>, S. I. Prokofiev<sup>a, \*\*</sup>, B. B. Straumal<sup>b, \*\*\*</sup>, and K. I. Kolesnikova<sup>b, \*\*\*\*</sup>

<sup>a</sup>Institute of Solid State Physics, Russian Academy of Sciences, Chernogolovka, Moscow oblast, 142432 Russia

<sup>b</sup>National University of Science and Technology MISiS, Moscow, 119049 Russia

\*e-mail: alenahas@issp.ac.ru

\*\*e-mail: prokof@issp.ac.ru

\*\*\*e-mail: straumal@issp.ac.ru

\*\*\*\*e-mail: kolesnikova@misis.ru

Received January 29, 2015; in final form, October 18, 2015; accepted for publication October 22, 2015

**Abstract**—The influence of temperature on the formation of the ( $\alpha$ Ti) grain-boundary interlayer in alloys Ti–2 wt % Co and Ti–4 wt % Co in the two-phase region ( $\alpha$ Ti) + ( $\beta$ Ti) of the Ti–Co phase diagram is studied in a temperature range of 690–810°C. The growth kinetics of the thickness ( $\Delta$ ) of the grain-boundary interlayer of the ( $\alpha$ Ti) phase in the Ti–2 wt % Co alloy is investigated at 750°C.  $\Delta$  depends on the annealing time as  $\sim t^{1/3}$ . The analysis of the results of experimental observations makes it possible to assume that an increase in  $\Delta$  is the manifestation of coalescence of ( $\alpha$ Ti), which is controlled by the bulk diffusion.

**Keywords:** titanium alloys, cobalt, decomposition of supersaturated solid solution, second phase precipitation, grain boundaries, kinetics, diffusion, coalescence

**DOI:** 10.3103/S1067821216070099

### INTRODUCTION

The formation of interlayers of the second phase at grain boundaries (GBs) strongly affects the mechanical properties of multiphase materials, in particular, titanium-based alloys, which are often subjected to quenching and aging for attaining high mechanical strength [1–4]. For example, the ( $\alpha$ Ti) phase often forms certain “fringes” in  $\alpha$ (Ti, Me) +  $\beta$ (Ti, Me) two-phase polycrystals of titanium alloys (Me are alloying elements in titanium) [5–8]. Such “fringes” of the second phase can substantially affect the properties of titanium and aluminum alloys, for example, their cutting workability [6], and promote the appearance of fracture cracks [8, 9]. We assume that the phase morphology in titanium alloys and, in particular, the formation of similar “fringes” can be determined not only by the bulk phase transitions [5, 7] but also by grain-boundary phase transformations [10, 11]. The second solid phase on the GB can either form continuous interlayers and consist of separate particles [11, 12]. Depending on temperature, equilibrium can correspond either to continuous interlayers and to particle chains [10, 13]. The kinetics of formation of GB second-phase interlayers is an important factor controlling the mechanical properties of alloys. Therefore, its study and the determination of the influence of the temperature on it have a large practical value since these results are used when selecting the thermal treat-

ment parameters providing the optimal characteristics of multiphase alloys.

The goal of this work is to investigate the influence of temperature and annealing time on the growth of GB interlayers in Ti–2 wt % Co and Ti–4 wt % Co alloys.

### EXPERIMENTAL

To prepare Ti–2 wt % Co and Ti–4 wt % Co alloys, we used titanium of TI-1 grade (99.9%) and cobalt (99.99%). The concentration of impurities in titanium TI-1 was as follows, wt %: Fe < 0.005, Si < 0.01, N < 0.002, C < 0.07, O < 0.01, and H < 0.01.

Alloys were smelted in an induction furnace in pure argon; then they were crystallized under rapid cooling. Cylindrical ( $\varnothing$ 10 mm) alloy ingots were structurally and chemically homogeneous over the length. They were cut into 5 mm thick wafers using a spark cutter. Their surface was ground and chemically treated to remove the damaged surface layer. Then some samples were sealed into evacuated quartz ampoules with a residual pressure of  $4 \times 10^{-4}$  Pa, and quenched in water. Annealing was performed in a temperature range of 690–810°C, i.e., in the ( $\alpha$ Ti) + ( $\beta$ Ti) two-phase region of the Ti–Co phase diagram [14]. The microstructural evolution kinetics was studied for the samples of the Ti–2 wt % Co alloy, which were annealed at 750°C for 45 min, 20 h, and 816 h. The

**Table 1.** Average thickness ( $2\Delta$ ) of GB interlayers and average size ( $R$ ) of the ( $\beta$ Ti) grains in the sample annealed according to various modes

Annealing parameters		Ti–2 wt % Co		Ti–4 wt % Co	
Temperature, °C	Time, h	$2\Delta$ , $\mu\text{m}$	$R$ , $\mu\text{m}$	$2\Delta$ , $\mu\text{m}$	$R$ , $\mu\text{m}$
Initial state		<0.5	–	–	–
690	720	24	151	24	188
	720	39	177	34	162
750	0.75	$5.2 \pm 0.3$	–	–	–
	20	$12.3 \pm 0.5$	–	–	–
	816	$42 \pm 1.0$	128	45	169
780	864	54	126	43	163
810	720	58	167	48	156

Undesignated errors of  $2\Delta$  does not exceed 5%.

**Table 2.** Lattice parameters of the phases and the ratio of the amount of phases in the Ti–4 wt % Co alloy before and after annealing at 780°C

Alloy state	$(\alpha\text{Ti})$			$(\beta\text{Ti})$	
	Fraction, %	Lattice parameters, nm		Fraction, %	Lattice parameters $a$ , nm
		$a$	$c$		
Before annealing	74.2	0.2952	0.4690	25.8	0.3205
After annealing	80.9	0.2955	0.4689	19.1	0.3201

parameters of all annealing procedures are presented in Table 1. Then the annealed samples were ground, mechanically polished, and chemically etched in a 1% aqueous HF solution to reveal the microstructure.

The microstructural investigations of the samples and quantitative thickness measurements of GB interlayers were performed using images made with a Neophot-32 optical microscope (Germany) equipped with a Canon Digital Rebel XT digital camera (Japan) (10 MPx). In particular, average grain size  $R = (S/\pi)^{1/2}$ , where  $S$  is the average grain area, and the average thickness ( $2\Delta$ ) of GB interlayers of the ( $\alpha$ Ti) phase were determined using microphotographs. The results of these measurements are presented in Table 1. If the resolution of optical images did not allow measuring the thickness of GB interlayers (in initial alloys and Ti–2 wt % Co alloys after short-term annealing procedures at 750°C), then images formed with the help of a Tescan Vega TS 5130 MM scanning electron microscope (Czech Republic) equipped with a LINK energy dispersive spectrometer (Oxford Instruments, Great Britain) were used for this purpose. This microscope was also used to determine the chemical composition of the samples revealed by probe scanning over their surface. The structural phase analysis was performed using a Siemens D-500 diffractometer (Germany) in  $\text{CuK}_{\alpha 1}$  radiation. The phase analysis and calculation of lattice parameters were performed in Pow-

derCell for Windows Version 2.4.08.03.2000 (Werner Kraus & Gert Nolze, BAM, Berlin).

## EXPERIMENTAL RESULTS

### *Microstructure of Initial Alloys*

Figure 1a shows the initial (before annealing) microstructure of the Ti–4 wt % Co alloy. It is formed by grains whose substructure consists of differently oriented colonies of alternating elongated lamellae of dark and light phases. The appearance of these colonies is the result of quenching the ingots of prepared alloys. The lamellar colonies are broken at the GB, and misorientation of lamellae allows us to clearly distinguish GBs coated with a thin dark phase layer in microphotographs. We failed to reliably determine the chemical composition of these phases because of high dispersity of the structure; however, it was established for the less disperse microstructure of alloys after annealing. The chemical and structural analysis of the dark and light phases showed that they are ( $\alpha$ Ti) and ( $\beta$ Ti), respectively, according to the Ti–Co phase diagram [14]. The structural analysis of the initial Ti–4 wt % Co alloy confirms this fact (Table 2). According to microanalysis, the average cobalt concentration in both alloys is close to that specified during their preparation. We note that their microstructures in the initial state are similar (Figs. 1a, 2a).

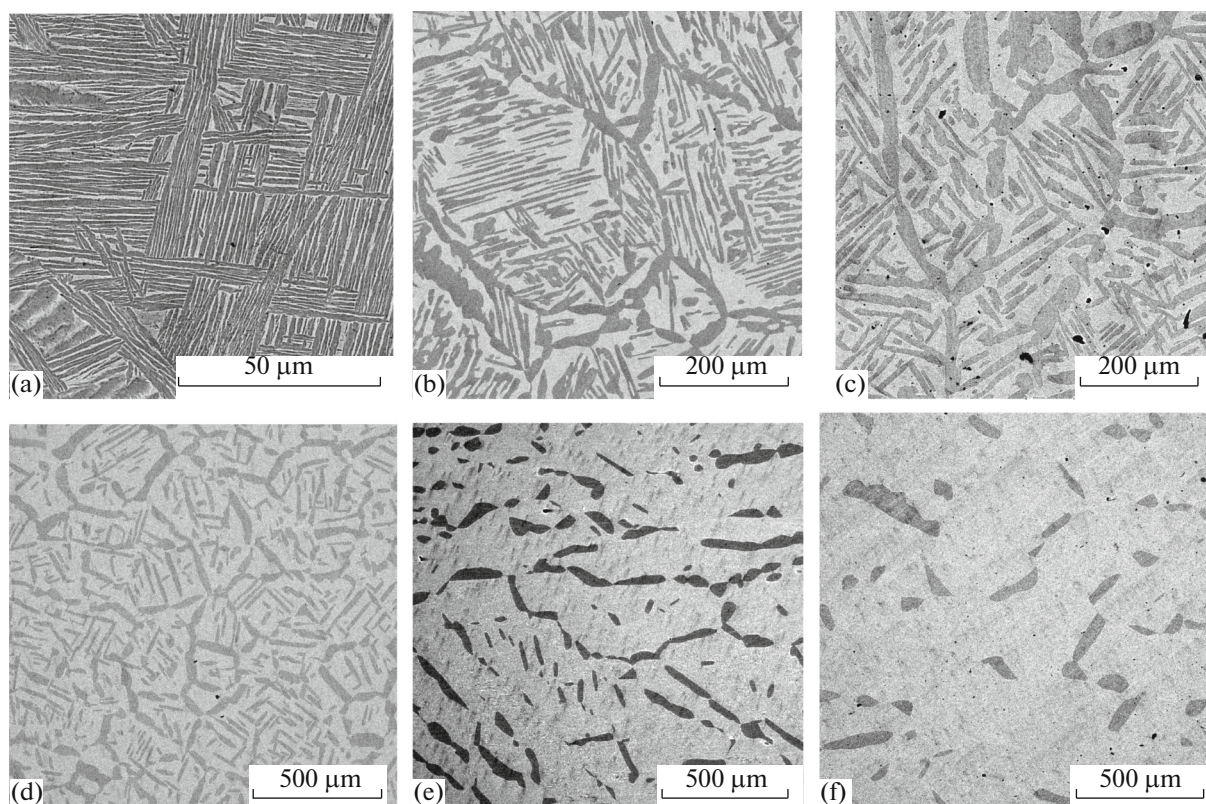


**Fig. 1.** Microstructure of (a) initial Ti–4 wt % Co alloy and (b–f) alloy at various temperatures (SEM).  $T$ , °C: (b) 690, (c) 720, (d) 750, (e) 780, and (f) 810. The ( $\alpha$ Ti) phase looks darker.

#### *Influence of the Annealing Temperature and Cobalt Content on the Alloy Microstructure*

It is established that annealing procedures lead to the destruction of the lamellar grain substructure (Fig. 1). Imperfection of ( $\alpha$ Ti) lamellas increases with an increase in the annealing temperature. They are broken, and bridges appear between the neighboring lamellas, after which lamellas are combined. In general, ( $\alpha$ Ti) lamellas thicken and become shorter with an increase in the annealing temperature. Microphotographs in Fig. 1 also show that ( $\alpha$ Ti) GB interlayers simultaneously thicken (see Table 1 as well), and boundaries free of ( $\alpha$ Ti) are formed in grains along them. The further increase in temperature causes the formation of isolated ( $\alpha$ Ti) inclusions incorporated into the matrix consisting of the ( $\beta$ Ti) light phase. We note that the light phase regions are inhomogeneous in microphotographs. They contain the substructure which is probably the result of the decay of ( $\beta$ Ti) when quenching annealed samples in water. This substructure consists of thin ( $\alpha$ Ti) and ( $\beta$ Ti) layers, which is confirmed by X-ray structural studies. Unfortunately, we failed to reliably determine the temperature dependence of the Co concentration in ( $\beta$ Ti) because of a high error. Almost the entire ( $\alpha$ Ti) phase is concentrated on the GB at highest temperatures (780 and 810°C) in the form of interlayers and/or separate GB

inclusions. The fraction of ( $\alpha$ Ti) decreases with an increase in temperature according to the phase diagram, which is especially clearly seen when comparing Figs. 1e and 1f.

In general, the observed changes in the microstructure can be considered as the manifestation of its coarsening. Since the coarsening kinetics, which is controlled by the bulk diffusion at sufficiently prolonged annealing times, is accelerated with an increase in temperature, several sequential stages of its evolution can be followed in the microphotographs of Fig. 1.

According to Table 1, the cobalt concentration in the alloy weakly affects the thickness of GB interlayers, and the average grain size varies insignificantly overall the studied temperature range.

#### *Influence of Annealing Duration at 750°C on the Microstructure of the Ti–2 wt % Co Alloy*

The analysis of Fig. 2 shows that the ( $\alpha$ Ti) regions inside the grain coarsen during annealing at 750°C with the simultaneous thickening of the ( $\alpha$ Ti) GB interlayers (see Table 1 as well). The character of microstructural changes upon the prolongation of the annealing time (Fig. 2d is especially clear) indicates the development of coarsening of the ( $\alpha$ Ti) particles with the process time (we considered above the coars-



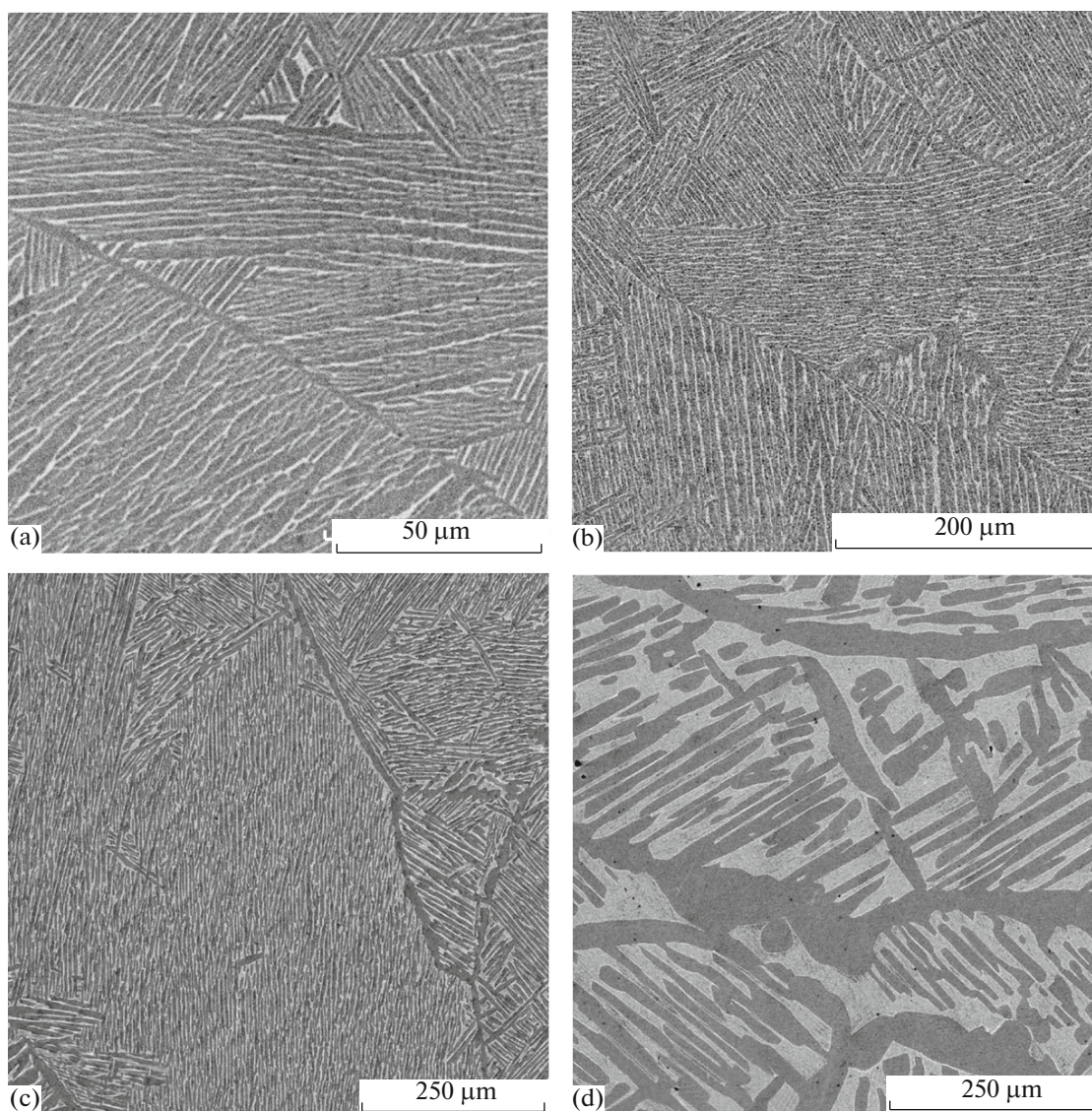


**Fig. 2.** Microphotographs (SEM) of (a) initial Ti–2 wt % Co alloy and (b–d) alloy annealed for various times at 750°C.  $t =$  (b) 45 min, (c) 20 h, and (d) 816 h. The ( $\alpha$ Ti) phase looks darker.

ening dynamics in the Ti–4 wt % Co alloy with an increase in the annealing temperature; see Fig. 1).

#### ANALYSIS AND DISCUSSION OF RESULTS

It is established (Fig. 3) that the average thickness of the ( $\alpha$ Ti) GB interlayers in the Ti–Co alloys under study increases with an increase in temperature. Annealing of the Ti–2 wt % Co alloy at  $T = 750^\circ\text{C}$  for 45 min, 20 h, and 816 h showed that the GB ( $\alpha$ Ti) interlayer becomes thicker with the prolongation of the annealing time (Table 1). To consider its growth kinetics, we plotted the time dependence of the average half-thickness of the ( $\alpha$ Ti) GB interlayer in log–log coordinates (Fig. 4). It is seen that its experimental points are approximated well by a straight line with a

slope of  $0.31 \pm 0.02$ , which is very close to the value of  $1/3$ . It is known that the growth kinetics of the second phase during the decomposition of the supersaturated solution, which is controlled by the bulk diffusion, usually follows parabolic law  $\Delta \sim t^{1/2}$  [15]. We note that this circumstance implies the initial chemical and structural homogeneity of the matrix. Indeed, it is known that the structural inhomogeneities of the matrix such as the GBs can lead to deviations from the parabolic growth law [15]. It was shown above that the grain substructure in the initial state (before annealing) consists of colonies containing ( $\alpha$ Ti) and ( $\beta$ Ti) lamellae and, consequently, ( $\alpha$ Ti)/( $\beta$ Ti) interfacial boundaries. It is natural to assume that the diffusion along the ( $\alpha$ Ti)/( $\beta$ Ti) interfacial boundaries can substantially contribute to the growth of ( $\alpha$ Ti) GB inter-

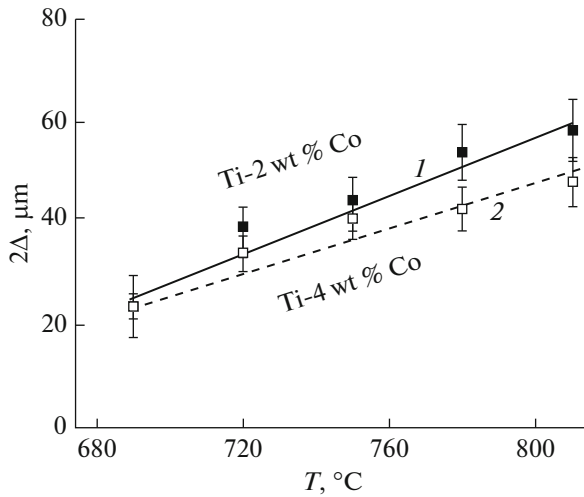


**Fig. 3.** Temperature dependence of the average thickness ( $2\Delta$ ) of the ( $\alpha$ Ti) GB interlayer in Ti-2 wt % Co (1) and Ti-4 wt % Co (2) alloys.

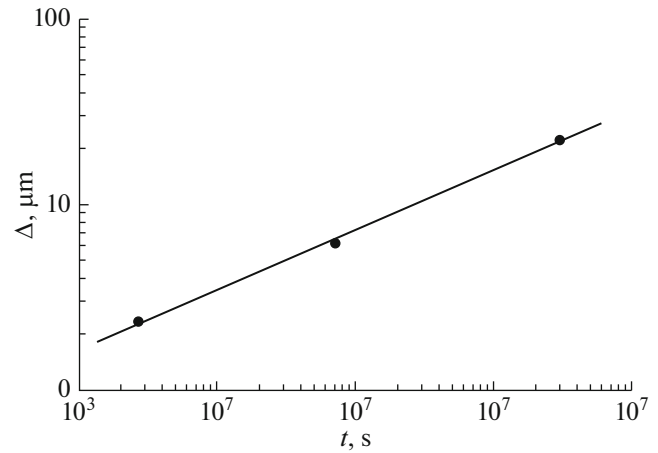


**Fig. 4.** Time dependence of the average half-thickness ( $\Delta$ ) of the ( $\alpha$ Ti) GB interlayer in the Ti-2 wt % Co alloy.

layers. Then the exponent of  $1/3$  can be governed by the time dependence of the effective interdiffusion coefficient ( $D_{\text{eff}}$ ), which can be associated with

(i) the variation in time of the relative contribution of the bulk and interfacial diffusion because of a decrease in the cobalt concentration gradient inside the grains with increasing time;

(ii) a decrease in density of interfacial boundaries and, consequently, their contribution to mass transfer as well as with the elongation of the average diffusion pathway to the interfacial boundary upon coarsening of ( $\alpha$ Ti) lamellas inside the grains with the annealing time;

(iii) lowering of the concentration gradient with the prolongation of the annealing time, which can lead to a decrease in  $D_{\text{eff}}$  owing to the possible concentration dependence of the interdiffusion coefficient.

These three factors can cause a decrease in  $D_{\text{eff}}$  with time. Under the assumption that  $\Delta \sim (D_{\text{eff}}t)^{1/2}$ , the expected time dependence of the effective interdiffusion coefficient has the form  $D_{\text{eff}} \sim t^{-1/3}$ .

We derived an expression which allows us to determine the effective interdiffusion coefficient from the data on the interlayer thickness of the growing GB  $\alpha$  phase and its growth time. For this purpose, we considered the growth of the  $\alpha$ -phase layer with concentration  $c_\alpha$  on the boundary of a spherical grain with radius  $R$  from the supersaturated solution with concentration  $c_0$  controlled by bulk diffusion ( $D_{\text{eff}}$ ). It is in equilibrium with the  $\beta$  phase (with concentration  $c_\beta$ ), which is formed at the  $\alpha/\beta$  interfacial boundary during the decomposition of the supersaturated solution, at the boundary of the GB  $\alpha$ -phase layer. It is supposed that  $D_{\text{eff}}$  is independent of the concentration.

The equation follows from matter balance at the  $\alpha/\beta$  interfacial boundary:

$$(c_\alpha - c_\beta) \frac{d\rho}{dt} = D_{\text{eff}} \left. \frac{\partial c}{\partial r} \right|_{r=\rho(t)}, \quad (1)$$

where  $\rho$  is the coordinate of the boundary of the  $\alpha$ -phase layer and  $r$  is the radial coordinate.

The diffusion inside the grain ( $\beta$  phase) is described as follows:

$$D_{\text{eff}} \frac{\partial c}{\partial \tau} = \frac{\partial^2 c}{\partial r^2} + \frac{2}{r} \frac{\partial c}{\partial r}, \quad (2)$$

with initial and boundary conditions  $c(r, t = 0) = c_0$ ,  $r \leq R$ , and  $c(\rho, t) = c_\beta$ .

The solution of the problem leads to the expression

$$D_{\text{eff}} = (R - \Delta)^2 / (4\lambda^2 t), \quad (3)$$

where, if we consider the cobalt concentration, parameter  $\lambda$  is determined by the equation

$$\sqrt{\pi} \lambda^3 \frac{\text{erfc}(\lambda)}{\exp(-\lambda^2)} - \lambda^2 + \frac{1}{2} \left( \frac{c_\beta^{\text{Co}} - c_0^{\text{Co}}}{c_\beta^{\text{Co}} - c_\alpha^{\text{Co}}} \right) = 0. \quad (4)$$

We calculated the values of the effective mutual diffusion coefficient from the experimental data for the samples of the Ti-2 wt % Co alloy annealed for various times at 750°C with the help of Eqs. (3) and (4). The time dependence of this characteristic in log-log coordinates having the slope of  $-1.04 \pm 0.01$  is shown in Fig. 5. Thus, dependence  $D_{\text{eff}} \sim t^{-1}$  rather than  $D_{\text{eff}} \sim t^{-1/3}$  takes place. It can be rewritten as  $(D_{\text{eff}}t)^{1/2} \approx \text{const}$ . This fact indicates that the GB interlayers grow much more slowly than is expected during the diffusion decomposition of the supersaturated solution.



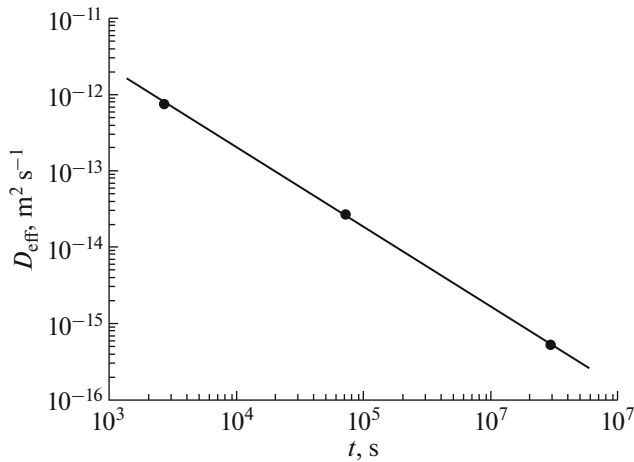


**Fig. 5.** Time dependence of the effective mutual diffusion coefficient found using Eqs. (3) and (4) from the data on the growth kinetics of the ( $\alpha$ Ti) GB interlayer in the Ti–2 wt % Co alloy at 750°C.

Consequently, the growth of ( $\alpha$ Ti) GBs is not associated with the decomposition of the supersaturated solution controlled by diffusion in the grain bulk and along ( $\alpha$ Ti)/( $\beta$ Ti) GBs. It is probably the result of coarsening of ( $\alpha$ Ti). Indeed, the area of interfacial boundaries and, consequently, the energy related to them decreases with an increase in thickness of GB interlayers. An increase in thickness of the GB interlayers caused by the decomposition of the ( $\beta$ Ti) supersaturated solution is probably unobservable since it is small and finishes after a short time because of the small thickness of ( $\alpha$ Ti) and ( $\beta$ Ti) lamellas in colonies.

Simultaneous coarsening in the grain bulk leads to spheroidization of lamella plates (in the absence of considerable anisotropy of the surface tension of interfacial boundaries). This process is accompanied by the development of shape instabilities of platelike lamellae. Shape instabilities are associated with the motion of lamella ends owing to the preferential dissolution and the development of thickness nonuniformity of the plates leading to their partition and connection of neighboring plates by necks [16]. The above-described peculiarities of shaping dynamics of lamellae with the prolongation of the annealing time can be seen in Fig. 2. Figure 1 shows similar changes in lamella shapes with an increase in the annealing temperature. We note that such behavior of lamellar structures during coarsening was observed previously in many studies, for example, in [17–20]. This fact gives us the basis to consider that an increase in thickness of ( $\alpha$ Ti) GB interlayers is caused precisely by coarsening. Indeed, the interfacial boundary associated with the GB interlayers of this grain has negative curvature on average for all grains, while the enveloping surface plotted around the lamella colony in the grain bulk, similarly to individual lamellae, has positive average curvature. This fact determines the driving force of the

growth of ( $\alpha$ Ti) GB interlayers, the final result of which is probably the purification of the grain bulk with respect to ( $\alpha$ Ti). It seems likely that the growth of GB interlayers occurs mainly owing to lamellas determining the shape of the enveloping surface and depends weakly on the kinetics of variation of the sizes and shape of other lamellas in the grain bulk.

Thus, it is established that the ( $\alpha$ Ti) GB interlayers thicken during coarsening controlled by bulk diffusion according to a law close to  $\Delta \sim t^{1/3}$ . The rise of the average size in the ensemble of spherical inclusions [21–23], in the ensemble of cylindrical inclusions [24, 25], and, as was shown by the authors of [26, 27] within the scope of the static self-similarity hypothesis, in the ensemble of inclusions with an arbitrary similar shape as well follows the same law.

## CONCLUSIONS

The influence of temperature and cobalt concentration on the formation of the ( $\alpha$ Ti) GB interlayer in Ti–2 wt % Co and Ti–4 wt % Co alloys in the ( $\alpha$ Ti) + ( $\beta$ Ti) two-phase region of the Ti–Co phase diagram is investigated in a temperature range of 690–810°C. The growth kinetics of the thickness of the ( $\alpha$ Ti) GB interlayer in the Ti–2 wt % Co alloy at 750°C is also investigated. These results allow us to conclude that the growth of ( $\alpha$ Ti) GB interlayers following the law  $\sim t^{1/3}$  is determined by the coarsening process controlled by diffusion in the grain bulk.

## ACKNOWLEDGMENTS

This study was supported by the Russian Foundation for Basic Research, project nos. 12-03-00894, 15-03-01127, and 15-53-06008, and by the Russian Federal Ministry for Education and Science (grant 14.A12.31.0001).

## REFERENCES

1. Il'in, A.A., Kolachev, B.A., and Pol'kin, I.S., *Titanovye splavy. Sostav, struktura, svoystva (Titanium Alloys. Composition, Structure and Properties)*, Moscow: VILS-MATI, 2009.
2. Kolachev, B.A., *Fizicheskoe metallovedenie titana (Physical Metallurgy of Titanium)*, Moscow: Metallurgiya, 1976.
3. Kolachev, B.A., Eliseev, Yu.S., Bratukhin, A.G., and Talalaev, V.D., *Titanovye splavy v konstruktivnykh i proizvodstve aviadvigately I aviatsionno-kosmicheskoi tekhniki (Titanium Alloys in Constructions and Production of Aeroengines and Aviation-and-Space Vehicles)*, Moscow: Moscow Aviats. Inst., 2001.
4. Kolachev, B.A., Betsofen, S.Ya., Bunin, L.A., and Volodin, V.A., *Fizikomekhanicheskiye svoystva legkikh konstruktivnykh splavov (Physical and Mechanical Properties of Light Structural Alloys)*, Moscow: Metallurgiya, 1995.

5. Kolachev, B.A. and Lyasotskaya, V.S., Correlation between diagrams of isothermal and anisothermal transformations and phase composition diagram of hardened titanium alloys, *Metal Sci. Heat Treat.*, 2003, vol. 45, pp. 119–126.
6. Egorova, Yu.B., Il'in, A.A., Kolachev, B.A., Nosov, V.K., and Mamonov, A.M., Effect of the structure on the cutability of titanium alloys, *Metal Sci. Heat Treat.*, 2003, vol. 45, pp. 134–139.
7. Kolachev, B.A., Veitsman, M.G., and Gus'kova, L.N., Structure and mechanical properties of annealed titanium alloys, *Metal Sci. Heat Treat.*, 1983, vol. 25, pp. 626–631.
8. Fishgoit, A.V., Maistrov, V.M., Ilin, A.A., and Rozanov, M.A., Interaction of short cracks with the structure of metals, *Sov. Mater. Sci.*, 1988, vol. 24, pp. 247–251.
9. Bobovnikov, V.N., Luk'yanenko, V.V., and Fishgoit, A.V., Effect of particles of the insoluble phase  $\alpha$ 9feni on the kinetics of fatigue crack propagation in alloy AK4-1, *Metal Sci. Heat Treat.*, 1982, vol. 24, pp. 191–194.
10. Straumal, B.B., Baretzky, B., Kogtenkova, O.A., Straumal, A.B., and Sidorenko, A.S., Wetting of grain boundaries in Al by the solid  $\text{Al}_3\text{Mg}_2$  phase, *J. Mater. Sci.*, 2010, vol. 45, pp. 2057–2061.
11. Straumal, B.B., Gust, W., and Watanabe, T., Tie lines of the grain boundary wetting phase transition in the Zn-rich part of the Zn–Sn phase diagram, *Mater. Sci. Forum*, 1999, vol. 294, pp. 411–414.
12. Straumal, B.B., Gornakova, A.S., Kucheev, Y.O., Baretzky, B., and Nekrasov, A.N., Grain boundary wetting by a second solid phase in the Zr–Nb alloys, *J. Mater. Eng. Perform.*, 2012, vol. 21, pp. 721–724.
13. Straumal, B.B., Gornakova, A.S., Kogtenkova, O.A., Protasova, S.G., Sursaeva, V.G., and Baretzky, B., Continuous and discontinuous grain boundary wetting in the Zn–Al system, *Phys. Rev. B*, 2008, vol. 78, p. 054202.
14. Murray, J.L., Diagrams of binary titanium alloys, *Bull. Alloy Phase Diagrams*, 1982, vol. 3 (1), pp. 74–85.
15. Gurov, K.P., Kartashkin, B.A., and Ugaste, Yu.E., *Vzaimnaya diffuziya v mnogofaznykh metallicheskih sistemakh (Interdiffusion in Multiphase Metallic Systems)*, Moscow: Nauka, 1981.
16. Sharma, G., Ramanujan, R.V., and Tiwari, G.P., Instability mechanisms in lamellar microstructures, *Acta Mater.*, 2000, vol. 48, pp. 875–889.
17. Graham, L.D. and Kraft, R.W., Coarsening of eutectic microstructures at elevated temperatures, *Trans. Metall. Soc. AIME*, 1966, vol. 236, pp. 94–96.
18. Tian, Y.L. and Kraft, R.W., Mechanisms of perlite spheroidization, *Metall. Trans. A*, 1987, vol. 18A, pp. 1403–1414.
19. Wey, M.Y. and Choi, J.H., Coarsening of lamellar microstructures, *J. Korean Inst. Met. Mater.*, 1994, vol. 32, pp. 1269–1273.
20. Park, D.-Y. and Yang, J.-M., Coarsening of lamellar microstructures in directionally solidified yttrium aluminate/alumina eutectic fiber, *J. Am. Ceram. Soc.*, 2001, vol. 84, pp. 2991–2996.
21. Lifshitz, I.M. and Slyozov, V.V., *O kinetike diffuzionnogo raspada peresyshchennykh tverdykh rastvorov* (On the kinetics of diffusion decomposition of supersaturated solid solutions), *Zh. Eksp. Teor. Fiz.*, 1958, vol. 35, pp. 479–492.
22. Wagner, C., Theorie der Älterung von Niederlagschlägen durch Umlösen (Ostwald-Reifung), *Z. Electrochem.*, 1961, vol. 65, pp. 581–591.
23. Ardell, A.J., Effect of volume fraction on particle coarsening—theoretical considerations, *Acta Metall.*, 1972, vol. 20, pp. 61–68.
24. Speich, G.R. and Oriani, R.A., Rate of coarsening of copper precipitate in an alpha-iron matrix, *Trans. Metall. Soc. AIME*, 1965, vol. 233, pp. 623–631.
25. Ardell, A.J., The growth of gamma prime precipitates in aged Ni–Ti alloys, *Metall. Mater. Trans. B*, 1970, vol. 1, pp. 525–534.
26. Mullins, W.W., The statistical self-similarity hypothesis in grain-growth and particle coarsening, *J. Appl. Phys.*, 1986, vol. 59, pp. 1341–1349.
27. Mullins, W.W. and Vinals, J., Self-similarity and growth-kinetics driven by surface free-energy reduction, *Acta Mater.*, 1989, vol. 37, pp. 991–997.

Translated by N. Korovin